npj | parkinson's disease

Article

Published in partnership with the Parkinson's Foundation

https://doi.org/10.1038/s41531-025-00963-8

# IC100 blocks inflammasome activation induced by α-synuclein aggregates and ASC specks



Brianna Cyr[1,6], Regina T. Vontell[2,3,6], Roey Hadad[1,4,6], Juan Pablo de Rivero Vaccari[1,4,5] & Robert W. Keane[1,4,5]

Parkinson's disease (PD) is associated with chronic sterile inflammation and persistent inflammasome activation involving α-synuclein and ASC protein aggregates, but the underlying mechanisms of the neuroinflammatory response remain unclear. Here, we used midbrain postmortem samples from donors with and without α-synucleinopathies to assess the expression of inflammasome proteins in patients with Parkinsonism. We show that dopaminergic neurons exhibit increased expression of ASC, NOD-like receptor protein (NLRP) 1, and modification of α-synuclein phosphorylation at serine129 (pS129) within the Lewy body inclusions, whereas NLRP3 was identified mainly in microglial. Moreover, treatment of LRRK2 cells with ASC specks from PD and Lewy body dementia patients induced inflammasome activation and cytotoxicity that was blocked by IC100. Administration of preformed α-synuclein aggregates to microglia resulted in a significant elevation in pS129, and this effect was also blocked by IC100. Thus, IC100 may be a promising therapeutic strategy for inflammatory disease modification in synucleinopathies and other diseases.

Lewy body dementia (LBD) and Parkinson's disease (PD) dementia are synucleinopathies that are associated with aggregations of misfolded α-synuclein that form Lewy bodies and Lewy neurites. Misfolded protein aggregates play a critical role in inflammasome activation and chronic inflammation that contribute to neurodegeneration in PD and Alzheimer's disease (AD), and a variety of proteinopathies[1–3]. In PD and other synucleinopathies, elevation of α-synuclein phosphorylated at serine129 (pS129) is considered a marker of pathology, and approximately 90% of aggregated α-synuclein in Lewy bodies contains pS129[4], indicating that a specific phosphorylation reaction is connected to pathology and may occur during neuronal activity[5]. Neuropathological changes of the distribution of Lewy bodies in PD have been characterized based on the progression of Lewy bodies, particularly in brain regions such as the brainstem, limbic structures, and the neocortex[6]. Importantly, in Braak stages 4 and 5, when the motor symptoms are evident, Lewy bodies are present moderately in the midbrain, and the loss of the normally pigmented neurons in the substantia nigra (SN) is mild to moderate, depending on size and maturation of the Lewy bodies to pale bodies[7].

In PD, chronic NLRP3 inflammasome activation is triggered by the accumulation of misfolded α-synuclein that results in the death of dopaminergic neurons[8]. Higher expression of inflammasome proteins NLRP3, ASC, and cleaved caspase-1 has been reported in postmortem brains of PD patients at the protein and mRNA levels[9–11]. Moreover, inflammasome proteins are highly elevated in the blood of PD and AD patients, indicating that chronic inflammasome activation may drive the pathology and further propagation of protein aggregates[12,13]. In addition, plasma samples from PD patients have significantly increased protein levels of oligomerized α-synuclein and IL-1β compared to healthy controls[14]. Furthermore, ASC specks are pathogenic protein aggregates that accumulate in the extracellular space, where they retain their ability to process pro-IL-1β[15] Extracellular ASC specks are phagocytosed by macrophages, resulting in lysosomal damage and IL-1β production[16].

Microglia are the CNS resident immune cells that respond to misfolded proteins, thereby activating the inflammasome. Microglia uptake α-synuclein aggregates released from neurons by mechanisms such as autophagy[17], phagocytosis[18], and endocytosis[19]. Moreover, ingested α-synuclein

[1]The Miami Project to Cure Paralysis, University of Miami Miller School of Medicine, Miami, FL, USA. [2]Department of Neurology, University of Miami Brain Endowment Bank, University of Miami Miller School of Medicine, Miami, FL, USA. [3]Evelyn F. McKnight Brain Institute, Department of Neurology, University of Miami Miller School of Medicine, Miami, FL, USA. [4]Department of Molecular Physiology and Cellular Biophysics, University of Miami Miller School of Medicine, Miami, FL, USA. [5]Department of Neurological Surgery, University of Miami Miller School of Medicine, Miami, FL, USA. [6]These authors contributed equally: Brianna Cyr, Regina T. Vontell, Roey Hadad. e-mail: rkeane@miami.edu

**Table 1 | Demographic data of patients used for histopathological analyses**

| PD Cases | Age (yr) | Sex | McKeith Score | PD Braak | Lewy body frequency in SN | Clinical duration of Parkinsonism (yrs) | AD neuropathological change | PMI (h) |
|---|---|---|---|---|---|---|---|---|
| 1 | 81 | M | 2 | 4 | Moderate | 10 | Low | 21 |
| 2 | 79 | M | 2 | 4 | Moderate | 19 | PART | 5 |
| 3 | 76 | M | 3 | 5 | Moderate | 15 | Intermediate | 21 |
| 4 | 81 | M | 3 | 5 | Frequent | 12 | Low | 19 |
| 5 | 85 | M | 3 | 5 | Frequent | 18 | PART | 8 |
| 6 | 71 | M | 3 | 5 | Frequent | 9 | Low | 24 |
| **Controls** | | | | | | | | |
| 1 | 93 | M | 0 | 0 | none | 0 | None | 18 |
| 2 | 54 | M | 0 | 0 | none | 0 | PART | 19 |
| 3 | 97 | M | 0 | 0 | none | 0 | Low | 22 |
| 4 | 63 | F | 0 | 0 | none | 0 | Low | 14 |
| 5 | 62 | M | 0 | 0 | none | 0 | Low | 26 |
| 6 | 67 | M | 0 | 0 | none | 0 | None | 16 |

*PD* Parkinson's disease, *yr* year, *M* male, *F* female, *PART* primary age-related tauopathy, *PMI* postmortem interval, *h* hour.

aggregates induce phosphorylation of intracellular α-synuclein in recipient cells[20], whereas excessive uptake of α-synuclein aggregates by microglia leads to production of inducible nitric oxide synthase (iNOS), thus altering microglia phenotype[21].

Microglia exposed to α-synuclein aggregates form F-actin-dependent intercellular networks to transfer α-synuclein fibrils to neighboring cells for degradation and clearance, which results in lowering the α-synuclein burden and attenuating the inflammatory profile in microglia[22]. Impairment of this process, as evidenced in PD mutations, leads to increased inflammatory profiles and cell death[22]. In PD and other synucleinopathies, the elevation of α-synuclein at serine129 (pS129) is widely used to assess pathology in terms of magnitude and extent of degeneration in humans and animal models[4]. However, recently it has been shown that phosphorylation of α-synuclein at pS129 occurs physiologically during neuronal activity, and it may be involved in synaptic activity, indicating a role beyond Lewy body pathology[5]. In addition, recent experimental evidence suggests that targeting α-synuclein aggregation may interfere with the deleterious proinflammatory responses in synucleinopathies[23].

Since inflammasome proteins have been shown to be elevated in PD patients, these proteins could be used as biomarkers to monitor disease progression and aid in diagnosis. Several PD animal model studies have demonstrated efficacy in therapeutic targeting of inflammasomes for disease modification in PD. These studies include: MCC950, a highly selective NLRP3 inhibitor[9,24], Glibenclamide[25], BAY11-7082, BOT-4-ene[26], 3,4-methylenedioxy-b-nitrostyrene[27], that interferes with ATPase activity of NLRP3 (132), and OTL1177 that inhibits NLRP3-ASC interactions[28]. Our group has developed IC100, a fully humanized mAb (IgG4κ) against ASC[29]. Previous studies using anti-ASC antibodies have shown that this therapeutic approach reduces pathology in several rodent models of excessive inflammasome activation in neural cells, such as spinal cord injury[30], traumatic brain injury[31], acute lung injury[32], multiple sclerosis[33], and inflammaging[34]. However, the efficacy of IC100 in PD has not been tested. Moreover, whether ASC specks from PD and LBD patients act as endogenous danger signals and induce inflammasome activation in human microglia or macrophages is yet to be studied. Therefore, we investigated the cell-type expression of inflammasome proteins in PD brains and whether ASC specks from PD and LBD patients are taken up by human microglia and induce inflammasome activation in culture. Moreover, we tested whether treatment with IC100 blocked inflammasome activation induced by ASC specks and significantly decreased the levels of pS129 after treatment with α-synuclein aggregates.

## Results

### Inflammasome signaling proteins are present in Lewy body formations

We first determined the distribution of Lewy bodies and the expression of inflammasome proteins ASC, NLRP1, and NLPR3 in postmortem human midbrain samples with and without α-synucleinopathies. Neuropathological changes and demographic data are shown in Table 1. Lewy bodies forming in the pigmented neurons of the SN were detected in various morphologies of formation using antibodies against α-synuclein. To determine whether aggregation of α-synuclein in Lewy body formation involved crosstalk with aggregation-prone ASC specks, we stained midbrain sections from cases assessed as PD Braak stages 4 and 5 with anti-human ASC (IC100) (Fig. 1). In the PD group, there were significantly less granular neurons identified in the SN ($p < 0.01$; PD 36 ± 11, $n = 6$; Control 72 ± 12, $n = 6$; Fig. 1F). The granular neurons in the SN presented varying degrees of ASC expression with morphological changes in the PD group (Supplementary Fig. 1). In neurons with minute formation of Lewy bodies, there were irregular granular pools of IC100 immunoreactivity present within melanin pigments (Fig. 1A). In addition, ASC was detected in neurons around the Lewy body (Fig. 1B) and pale body (Fig. 1C) formations in brain sections corresponding to the active phosphorylation of α-synuclein. Furthermore, in the control group, a low level of expression of ASC was evident in a few neurons showing a granular pattern (Fig. 1D), but the majority of neurons were negative for ASC (Fig. 1E). Therefore, it appears that Lewy bodies are surrounded by ASC specks at various disease stages of formation.

Next, we evaluated the distribution of ASC in Lewy bodies that were immunoreactivity for pS129 α-synuclein and determined the morphology of the microglia that were proximal to the Lewy bodies. Perinuclear IC100 immunoreactivity in neurons was seen in cases with or without PD pathology. In cases of PD, the LBs were delineated with a mouse monoclonal α-synuclein and were surrounded by ameboid-shaped microglia (Fig. 1G, Gi, Gii). IC100 colocalized with α-synuclein (Fig. 1Giii), but IC100 immunoreactivity was not as dispersed as the α-synuclein expression (Fig. 1Giii). α-synuclein was not detected in neurons (Fig. 1H, Hi) of the SN or in microglial cell bodies (Fig. 1Hii) in the control groups, and IC100 distribution was more diffusely spread in the cytoplasm of SN neurons in controls, and microglia had more ramified or surveying morphology (Fig. 1H, Hiii).

### Microglia express NLRP3 whereas NLRP1, ASC (IC100), and pS129 α-synuclein is present in pale bodies

Previous studies have reported that NLRP1 and ASC (identified by IC100, that is directed against the PYD domain of ASC) expression colocalized in neurons with tauopathies in cases with AD[35]. In addition, caspase-1 was

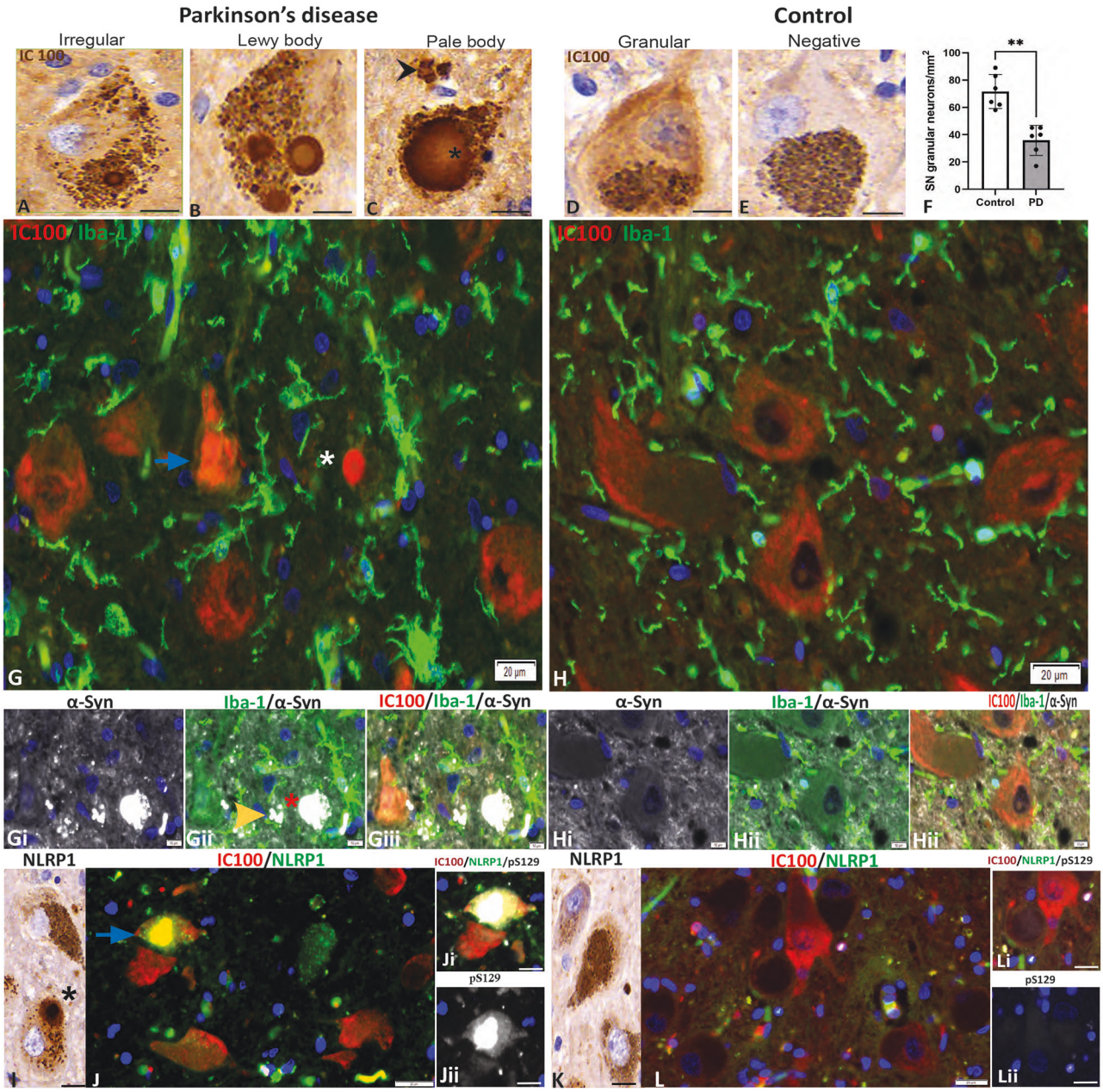


**Fig. 1 | Characterization of ASC (IC100) accumulation in ASC and NLRP1 speck formation in neurons with Lewy body pathology.** ASC expression and accumulation vary in different morphologies of Lewy body formation. PD sections presented with different forms of Lewy body pathologies; irregular-shaped (**A**), Lewy bodies (**B**), pale bodies (**C**; black asterisk) and free neuromelanin (**C**; black arrowhead) were stained with human anti-ASC antibody (IC100, black asterisks) in the SN of PD donors and controls (**D** and **E**). A significant reduction of SN granular was seen in PD donors compared to controls (**F**). In (**G**), IC100 immunostaining is present as granular/widespread in dopaminergic neurons (blue arrow) or within the intracellular Lewy body formation (white asterisk). Mouse anti-α-synuclein (Clone 42) is present in Lewy body fragments (**Gi–Giii**); white (red) asterisk marks where the Lewy body formed in neuron seen in image (**G**) in neurons and in ameboid-shaped microglia (**Gii**, green; yellow arrow). **H** IC100 (red) distribution in control dopaminergic neurons in the SN. α-Synuclein staining in white matter tracts (**Hi**; white) but not in microglia (**Hii**; green) or neurons that show granular IC100 immunostaining (**Hiii**; green). NLRP1 is present in Lewy body clusters (**I**) in donors with PD pathology, but not in controls (**K**). IC100 colocalized with NLRP1 (**J**; Blue arrow and **Ji**) in neurons that were positive for pSer129 α-synuclein (**Jii**). **L**, **Li**, and **Lii** correspond to controls that present few neurons with cytoplasmic IC100. mm = millimeter; $^{**}p < 0.01$; α-Syn = alpha synuclein; Adapter protein apoptosis-associated speck-like protein containing a caspase recruitment domain (ASC); Substantia nigra (SN). Scale bars = 10 µm (**A–E**, **Gi–Giii**, **Hi–Hiii**, **I**, **Ji**, **Jii**, **K**, **Li**, and **Lii**) and 20 µm (**G**, **H**, **J**, and **L**).

found in the core of Lewy bodies extracted from human PD patients' brains[36]. Therefore, we aimed to establish the expression patterns of NLRP1, NLRP3, ASC, and pS129 α-synuclein in SN neurons in Lewy body pathology (Fig. 2). Triple-labeling immunohistochemistry of PD sections was performed using mouse anti-NLRP1, human anti-ASC (IC100), and rabbit anti-pSer129 α-synuclein. NLRP1 expression was evident in irregular-shaped neurons and peripheral Lewy bodies that circumvented the pale body (Fig. 1I, J). In addition, NLRP1 colocalized with ASC in neurons that had Lewy bodies in the periphery to the formation of pale bodies (Fig. 1Ji, Jiii). In controls, there was light granular staining of NLRP1 (Fig. 1K), and cytoplasmic IC100 immunoreactivity was seen in a few neurons (Fig. 1L), but there was no neuronal co-expression of NLRP1 and pSer129 α-synuclein (Fig. 1Li, Lii). Thus, it appears that NLRP1 and ASC colocalize with pSer129 in the Lewy bodies.

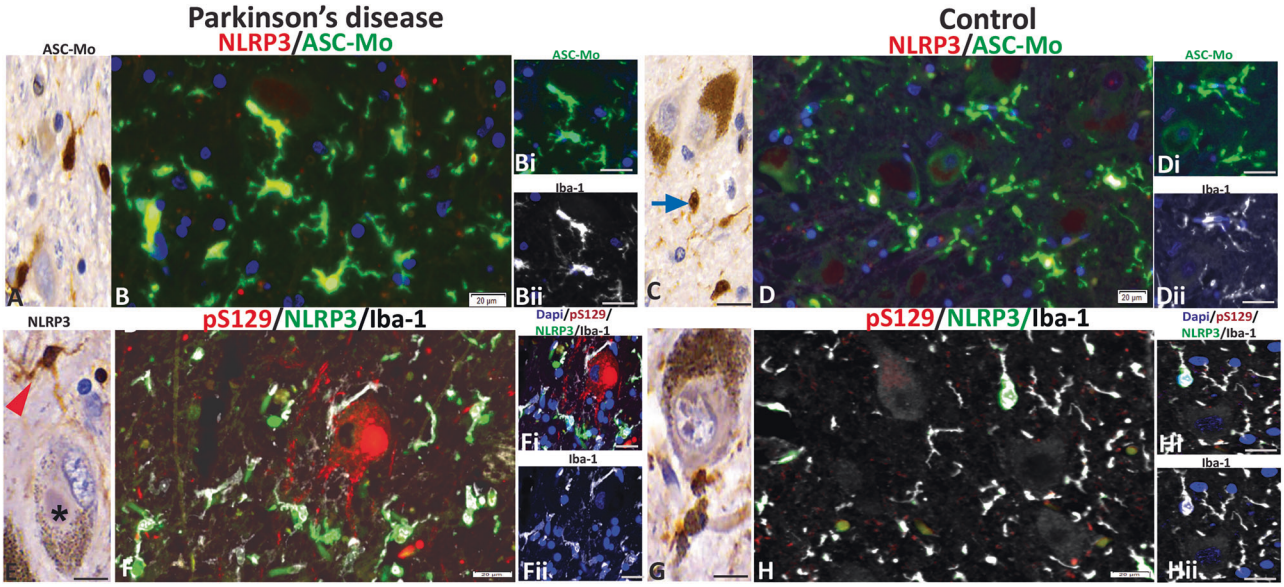


**Fig. 2 | Localization of NLRP3 with ASC in microglia with and without Lewy body pathology.** Mouse monoclonal ASC (B-3) stains microglia around Lewy body clusters (**A**) in donors with PD pathology and in controls (**C**). ASC colocalized with NLRP3 (**B**) in microglia that were positive Iba-1 (**Bii**). **D**, **Di**, and **Dii** correspond to controls that present microglia with nuclear ASC and NLRP3 expression. NLRP3 immunoreactivity is present in microglia-like cells (**E**; red arrowhead) that are adjacent to a neuron with a pale body (black asterisk) and in the microglia of controls (**G**) around neurons with melanin pigment. Lewy bodies detected using pSer129 show frequent Iba-1$^+$ microglia (**Fiii**) that also express NLRP3 (**F** and **Fi**), whereas in controls, there were a sparse amount Iba-1$^+$ microglia (**Hii**) that are positive for NLRP3, while neurons did not reveal pSer129 immunoreactivity (**H** and **Hi**). Adapter protein apoptosis-associated speck-like protein containing a caspase recruitment domain (ASC); Substantia nigra (SN); alpha (α); Scale bars = 10 µm (**A**, **Bi**, **Bii**, **C**, **Di**, **Dii**, **E**, **Fi**, **Fii**, **G**, **H**, **Hi**, and **Hii**) and 20 µm (**B**, **D**, **F**, and **H**).

### Microglia express NLRP3 and ASC

Next, we performed triple immunolabeling for ASC using a mouse monoclonal antibody raised against the CARD domain and the microglial marker Iba-1, as well as NLRP3, and pSer129. The mouse monoclonal anti-ASC antibody was detected in microglia in PD cases (Fig. 2A, B) and in controls (Fig. 2C, D). Moreover, we identified that ASC and NLRP3 expression were evident in Iba-1$^+$ microglia in PD cases (Fig. 2B, Bi, Bii) and in the controls (Fig. 2D, Di, Dii). NLRP3 staining was detected in the majority of microglia that surrounded neurons with Lewy body formations (Fig. 2E), and these microglia also co-expressed pSer129 α-synuclein (Fig. 2F, Fi, Fii). In controls, NLPR3$^+$ protein expression in microglia was weak (Fig. 2G, H, Hi), and these neurons were negative for pSer129 α-synuclein (Fig. 2Hii).

### ASC specks induce inflammasome activation and cell death in microglia in a dose-dependent manner

Previous studies have reported that macrophages phagocytose ASC specks[16,27]. Therefore, we first isolated ASC-citrine-labeled specks from the brains of ASC-citrine reporter mice and administered them to human HMC3 microglia in culture to assess whether microglia ingest extracellular ASC specks. As shown in Fig. 3A, numerous citrine-ASC aggregates were visible within the cytoplasm of microglia after 1.5 h of exposure, indicating that human microglia, like macrophages, phagocytize ASC specks.

ASC specks activate the inflammasome in immune cells[16,27] that results in pyroptosis[9]. Therefore, we measured inflammasome activation and cell death *via* caspase-1 activity and lactose dehydrogenase (LDH) release, respectively, after ASC speck administration to WT microglia. There was a significant increase in caspase-1 activity (Fig. 3B) and LDH release (Fig. 3C) in microglial cells at a concentration of 200 µg/mL of extracellular ASC specks and higher. Furthermore, to determine whether this concentration of ASC specks is physiologically relevant, we measured the concentration of ASC released into the media (Supplementary Fig. 2A) as well as caspase-1 activity (Supplementary Fig. 2B) following LPS + ATP stimulation of microglia. The concentration of ASC released into the media was higher than the amount of extracellular ASC specks we administered to the cells, and this finding was consistent with increased activity of caspase-1. Furthermore, a group of cells was pretreated with IC100 and resulting in significantly lower levels of ASC released and caspase-1 activity. Thus, these results suggest that ASC specks induce inflammasome activation and cell death in human microglia.

### Serum-derived ASC specks from PD patients activate the inflammasome in WT LRRK2 parental RAW 264.7 cells, leading to cell death

Our previous work has shown that inflammasome proteins are highly elevated in the blood of PD patients[13], indicating that inflammasome proteins are present extracellularly in PD. Thus, to determine whether extracellular ASC specks induce inflammasome activation in macrophages leading to cell death, we isolated protein aggregates by partial purification of the pyroptosome from the serum of healthy subjects and PD patients and analyzed oligomerization of ASC by immunoblotting procedures (Fig. 4A). ASC aggregates from PD subject showed an increase in dimers and oligomers compared to healthy controls, indicating increased ASC speck formation in the cells that were challenged with protein aggregates from PD patients (Fig. 4A). Next, we evaluated whether these ASC specks induced cell death (Fig. 4B) and inflammasome activation (Fig. 4C, D). ASC specks from PD patients significantly induced cytotoxicity in human microglia compared to healthy controls as evidence by significant release of LDH (Fig. 4B). In addition, ASC specks from PD patients caused significantly higher levels of caspase-1 than aggregates from healthy controls (Fig. 4C). We then tested the efficacy of IC100 to block caspase-1 activation by adding 50 µg/mL of IC100 for 30 min prior the exposure to ASC aggregates (Fig. 4D). IC100 significantly decreased inflammasome activation induced by serum-derived ASC specks from PD patients (Fig. 4D). These results demonstrate that IC100 significantly blocks inflammasome activation and cytotoxicity in LRRK2 parental RAW 264.7 cells induced by serum-derived ASC specks from PD.

### IC100 blocks inflammasome activation in LRRK2 parental RAW 264.7 cells treated with brain-derived ASC specks from LBD patients

Next, we evaluated whether brain-derived ASC aggregates from LBD patients induce inflammasome activation in macrophages. Cells were

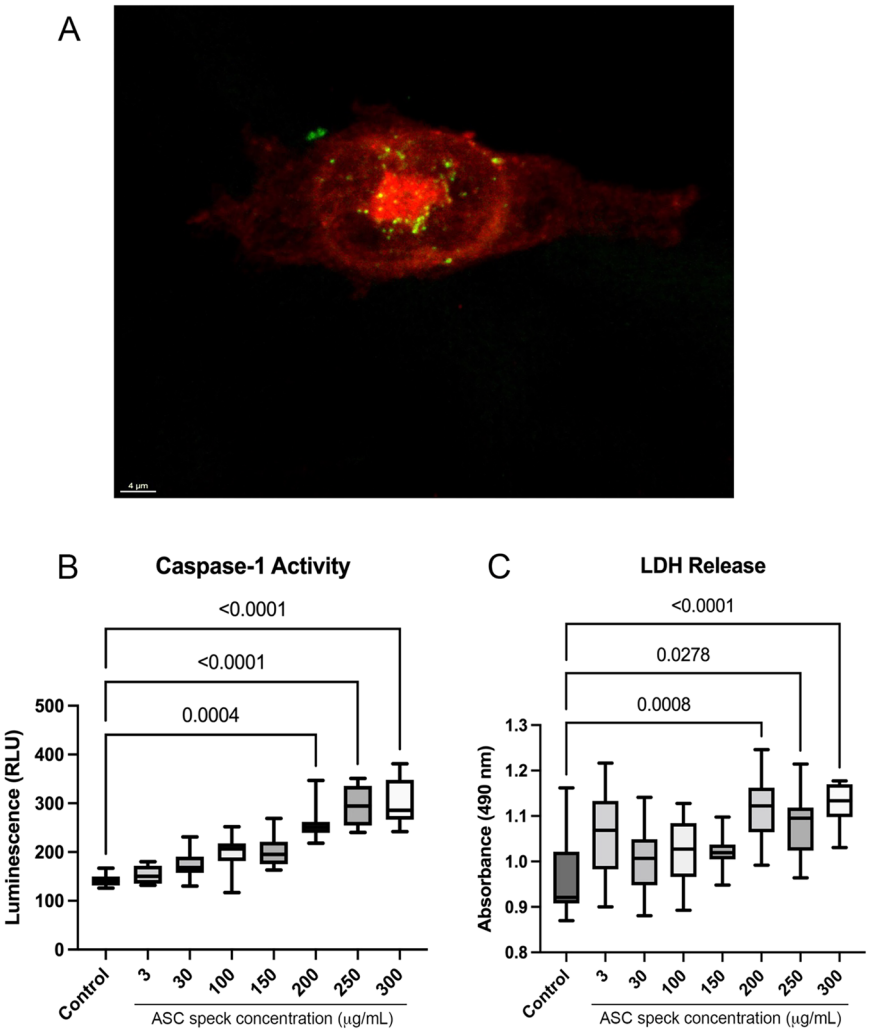


**Fig. 3 | Microglia uptake of extracellular ASC specks induces inflammasome activation and cell death. A** ASC specks isolated from R26-CAG-ASC-citrine brain protein lysates (green) were administered to HMC3 microglia (red) in culture. Scale bar = 4 µm. Microglia were treated with increasing concentrations of ASC specks isolated from C57BL/6 J brain protein lysates. Caspase-1 activity (**B**) and lactate dehydrogenase (LDH) release (**C**) were measured in the media. Data presented as boxes with the 5th and 95th percentiles. $N = 6–12$ per group.

treated with 3 different concentrations of ASC specks (0.05, 0.5 and 5.0 µg/mL) (Fig. 5). All concentrations of ASC specks tested significantly induced inflammasome activation (Fig. 5A). We then tested the efficacy of IC100 to block inflammasome activation by treating cells with 5 and 50 µg/mL of IC100 for 30 min prior to addition of 0.05 µg/mL of ASC specks. IC100 significantly decreased inflammasome activation induced by brain-derived ASC specks from LBD patients (Fig. 5B). These results demonstrate that IC100 significantly blocks inflammasome activation and cytotoxicity in LRRK2 parental RAW 264.7 cells induced by brain-derived ASC specks from LBD.

### IC100 decreases phosphorylation of α-synuclein and alters the cellular distribution of pS129 in human microglia

It has been established that human microglia uptake α-synuclein aggregates, resulting in phosphorylation of intracellular α-synuclein[20], whereas excessive uptake of α-synuclein aggregates by microglia results in induction of an aberrant human microglia phenotype[21].To establish the effects of fibrillary α-synuclein on the levels of total α-synuclein and pS129, we treated HMC3 cells with an excess of α-synuclein preformed fibrils (7 mM) for 3 days. In addition, a group of cells was treated with IC100 (10 µg/mL) alone or in combination with 7 mM α-synuclein preformed fibrils (Fig. 6). Controls were left untreated. We first tested the fibrillary formation of α-synuclein by a thioflavin T (ThT) assay (Supplementary Fig. 3) to corroborate that the α-synuclein used in this study corresponded to the fibrillary form of α-synuclein. Cells were harvested and protein lysates were analyzed by immunoblotting (Fig. 6). Treatment with α-synuclein preformed fibrils induced a significant increase in caspase-1 activity (Fig. 6A) and release of IL-1β from HMC3 cells, and both effects were significantly reduced by IC100 (Fig. 6B). The total levels of α-synuclein were unchanged by 3 days of treatment with 7 mM preformed fibrils, even with the administration of IC100 (Fig. 6C, D). However, IC100 treatment significantly lowered the levels of pS129 after 3 days of exposure (Fig. 6C, E), indicating that IC100 interferes with α-synuclein S129 phosphorylation induced by α-synuclein aggregates.

To study the distribution of pS129 after treatment with α-synuclein preformed fibrils, we treated microglia with α-synuclein preformed fibrils in the presence and absence of IC100 and examined the cellular distribution of pS129 by confocal microscopy. Control cells exhibited weak punctate immunoreactivity that was distributed throughout the cell (Fig. 6F). Human microglia treated with α-synuclein preformed fibrils for 3 days showed increased pS129 immunoreactivity, and examination of super-resolution images revealed intense pS129 immunoreactivity throughout the cell. In contrast, HMC3 cells treated with α-synuclein preformed fibrils + IC100 exhibited less intense pS129 immunoreactivity that was largely localized near the plasma membrane (Fig. 6F, arrow). Together, these results indicate that IC100 decreases pS129 levels after treatment with α-synuclein preformed fibrils and alters the cellular distribution pattern in human microglia.

## Discussion

Chronic immune and inflammasome activation induced by accumulated misfolded protein aggregates, such as ASC specks and α-synuclein

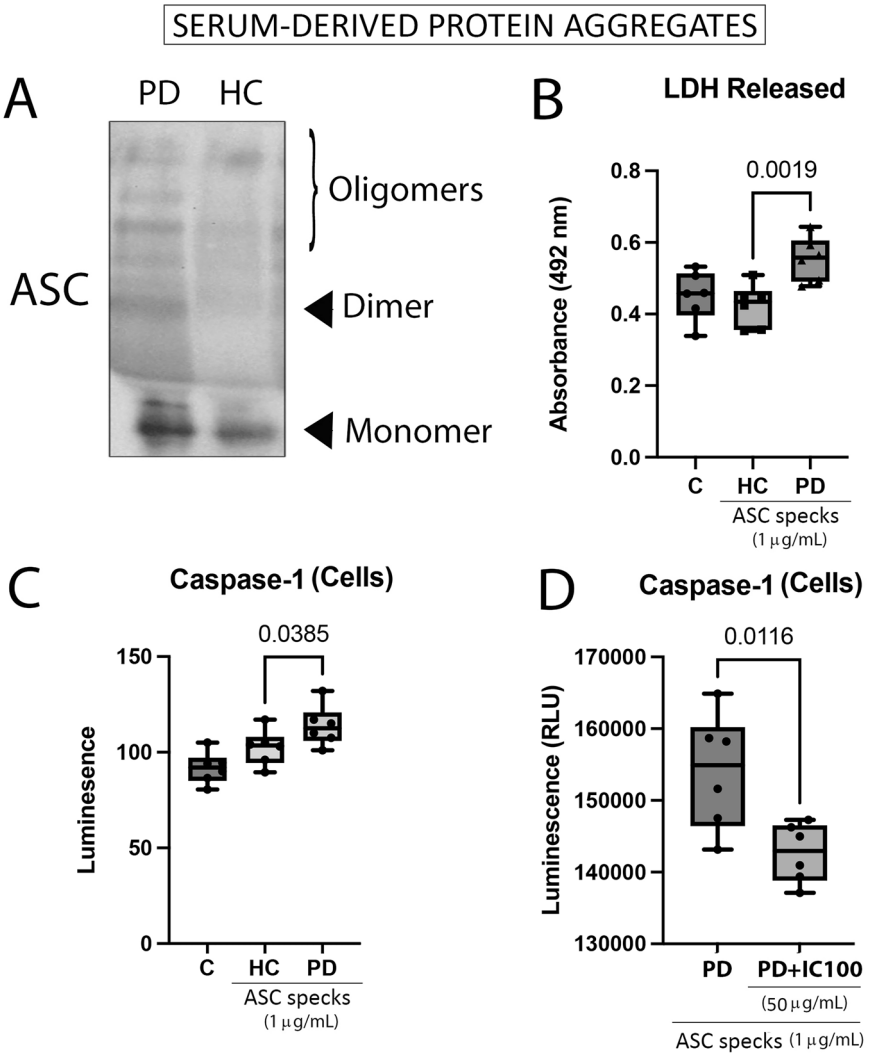


**Fig. 4 | Serum-derived ASC specks activate the inflammasome in LRRK2 cells. A** Representative immunoblot of ASC oligomerization isolated from the serum of PD patients and HC. LRRK2 parental RAW 264.7 cells were treated with ASC specks derived from the serum of PD patients and HC and measured for LDH release in the media (**B**) and caspase-1 activity in the cells (**C**). A group of cells was pretreated with IC100 prior to PD-derived ASC speck administration, and caspase-1 activity was measured in cells (**D**). Data presented as boxes with the min and max showing all data points. $N = 6$ per group. Parkinson's disease (PD); healthy control (HC); Apoptosis-associated speck-like protein containing a caspase recruitment domain (ASC); Lactose dehydrogenase (LDH).

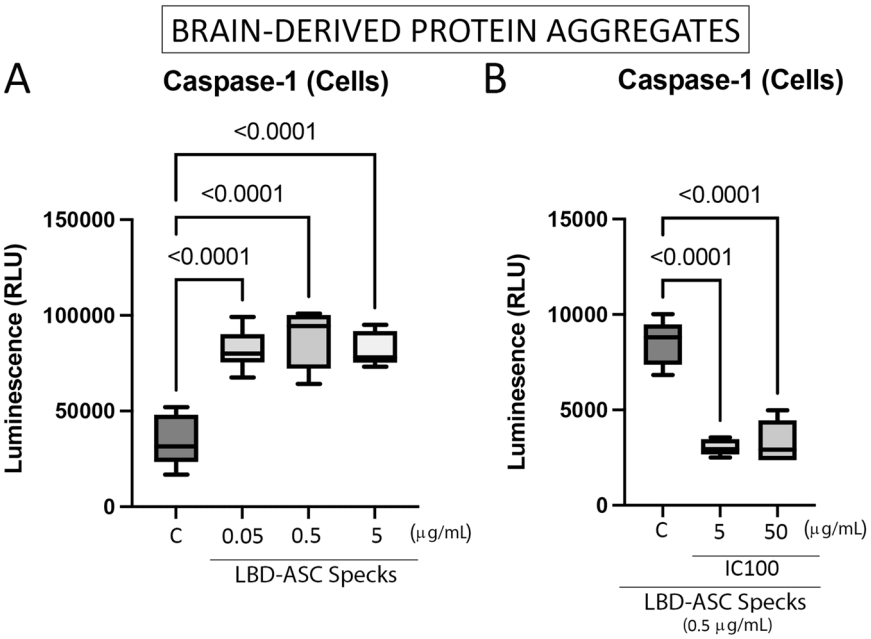


**Fig. 5 | IC100 blocks inflammasome activation in LRRK2 treated with serum-derived ASC specks from LBD patients. A** LRRK2 parental RAW 264.7 cells were administered ASC specks derived from the brains of LBD patients in increasing concentrations (0.05, 0.5, and 5 μg/mL), and caspase-1 activity in cells was measured. **B** LRRK2 parental RAW 264.7 cells were pretreated with IC100 prior to administration of 0.5 μg/mL LBD-derived ASC specks, and caspase-1 activity was measured in the cells. Data presented as boxes with the 5th and 95th percentiles. $N = 6$ to 12 per group. Lewy body disease (LBD); Apoptosis-associated speck-like protein containing a caspase recruitment domain (ASC).

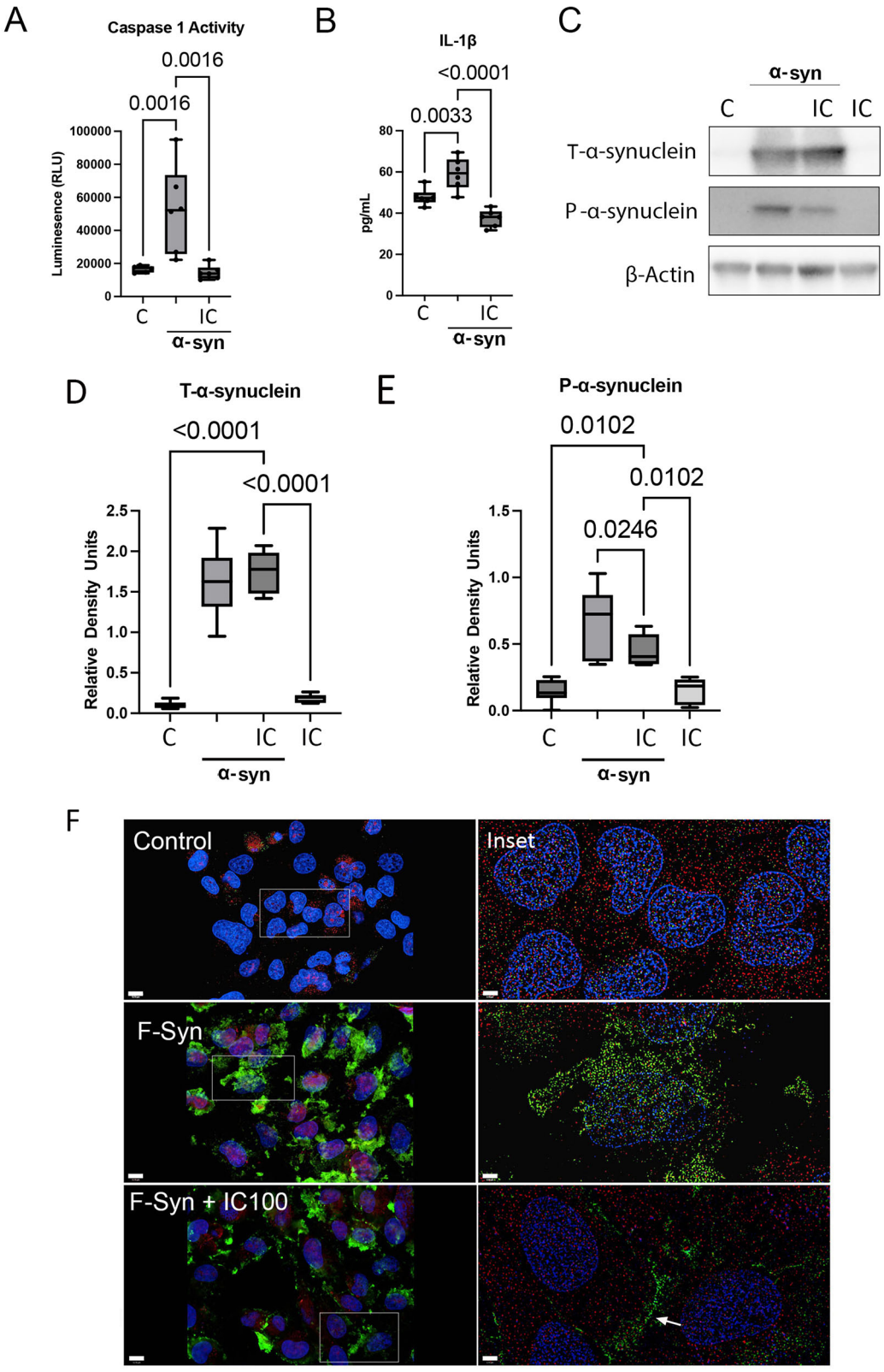


preformed fibrils, are key pathological mechanisms that drive neurodegeneration in PD, AD, and other neurological diseases[37]. In this study, we demonstrate that there was a loss of granular neurons in postmortem cases with PD pathological changes. We found that in LB and Lewy neurites, the inflammasome proteins NLRP1, ASC, and pSer129 α-synuclein are present in LB neurons of PD subjects when using an ASC antibody raised against the PYD domain. In addition, we show that NLRP3 and ASC are seen in microglia using a commercially available ASC antibody raised against the CARD domain and present more activated morphology in PD pathology. Moreover, α-synuclein preformed fibrils significantly increased levels of total α-synuclein and pS129, and ASC specks from PD and LB patients trigger inflammasome activation that is inhibited by treatment with IC100.

**Fig. 6 | IC100 inhibits inflammasome activation after exposure to α-synuclein preformed fibrils.** IC100 inhibits caspase-1 activity (**A**) and IL-1β (**B**) release in HMC3 microglia treated with α-synuclein preformed fibrils. HMC3 cells were treated with LPS alone or treated with LPS + 7 μm α-synuclein preformed fibrils or LPS + 7 μm α-synuclein preformed fibrils + 1 μg/mL IC100 for 24 h. Caspase-1 activity was determined using the Caspase-Glo 1 assay, and IL-1β was determined by ELICA. Data presented as boxes with the min and max showing all data points. $N = 6$ per group. Representative immunoblots (**C**) and quantification (**D**) of total α-synuclein preformed fibrils and pSer129 of human HMC3 microglia treated with 7 μM α-synuclein preformed fibrils with and without IC100 (10 μg/mL) for 72 h. Although IC100 did not alter the levels of total a-synuclein (**C**, **D**), it significantly lowered the protein levels of pSer129 (**C**, **E**). Data presented as boxes with the min and max showing all data points. $N = 6$ per group. **F** Confocal images showing that IC100 decreases pSer129 expression in human microglia. Human microglia were treated with α-synuclein preformed fibrils for 72 with and without IC100 (10 μg/mL) and stained for pSer129 (green), ASC (red), and DAPI (blue). Controls were left untreated. Super resolution of the inset is shown in the right panels. IC100-treated cells presented decreased immunoreactivity of pSer129 but did not alter the expression of ASC. Scale bars: Left Panels = 12.76 μm, Right Panels = 3.19 μm.

In addition, IC100 treatment altered the cellular distribution of pSer129 and decreased levels of pSer129, indicating improvement in pathogenic α-synuclein clearance.

Inflammasome activation has been reported in the dopaminergic system in PD patients[9,10], in blood[13], and mucosal samples[11,13]. Human PD patients have elevated levels of NLRP3, ASC, and caspase-1 primarily localized in microglia of the SN, and elevated levels of extracellular ASC are present in the serum of PD and LB patients[9,12,13]. Moreover, insoluble α-synuclein preformed fibrils induce monocytes[38] and microglia[39] to release IL-1β following NLRP3 inflammasome activation. In a recent study, a direct relationship between ASC protein levels and misfolded α-synuclein was found in PD mouse brains[40]. ASC specks amplified NLRP3 inflammasome activation induced by α-synuclein stimulation, which heightened reactive microgliosis and increased dopaminergic degeneration and motor deficits, suggesting that ASC specks contribute to the propagation of inflammasome activation.

Extracellular ASC specks are present in neurodegenerative diseases[37]. ASC specks have extracellular and prionoid activities[16], and upon release, remain active in the extracellular space where they are taken up by recipient cells and propagate the inflammatory response[16]. Here, we demonstrate that ASC and NLRP1 are present in the core of α-synuclein Lewy bodies. This finding suggests that aggregation-prone proteins involved in PD and the inflammasome may exacerbate neurodegeneration in PD. In a recent animal study of PD, ASC levels positively correlated with disease progression, in which an increase in the number of ASC specks correlated with α-synuclein pathology, suggesting that ASC may be involved in the propagation of inflammasome-mediated pathology triggered by α-synuclein preformed fibrils. Together, our findings establish that ASC aggregates from PD and LBD patients act as triggers of inflammasome activation. Importantly, treatment with IC100 significantly blocked inflammasome activation by ASC aggregates from PD and LBD patients, indicating that targeting ASC may be effective as a potential therapy for PD and LBD. Whether these protein aggregates mediate and influence co-morbidities associated with CNS degeneration in PD and LBD remains to be determined.

Lewy body pathology is are inclusion bodies of abnormal aggregates of α-synuclein and a multitude of proteins that develop inside the nerve cells, which can result in Parkinsonian symptoms when inclusions progress in the dopaminergic neurons of SN neurons in the midbrain. Lewy bodies are protein inclusions of at least 95 different proteins[7,41]. PD patients have elevated levels of NLRP3, ASC, and caspase-1 in serum and are present in microglia in the SN[9,12]. Caspase-1 is predominantly present in the core of Lewy bodies extracted from human PD patients' brains, which is surrounded by α-synuclein[42]. Our findings that LBs contain NLRP1 and ASC suggest that inflammasome proteins and protein aggregates in PD may cross-seed. The nanoscale organization of the endogenous ASC speck has been determined using a variety of fluorescence microscopy approaches, including super-resolution microscopy, and the speck contains a dense core with filaments protruding from the center of the speck[43]. ASC specks have been reported to co-aggregate cytosolic proteins on their surface through non-specific protein interactions[44]. Thus, it is possible that there is a crosstalk between ASC and NLRP1 in neurons and neuron-derived α-synuclein aggregates in PD to generate Lewy bodies in PD and Lewy body dementia.

α-Synuclein is a peripheral membrane protein that associates with synaptic vesicles and membranes[45]. Approximately 90% of α-synuclein in Lewy bodies is phosphorylated at serine129. Internalization of α-synuclein preformed fibrils is a key step in the propagation of α-synuclein aggregates. Furthermore, several processes have been linked to the uptake of α-synuclein preformed fibrils, such as lymphocyte-activated gene 3 (LAG3) uptake[46], autophagy[17], phagocytosis[18], and endocytosis[19]. Moreover, the seed-dependent formation of α-synuclein with prion-like aggregation requires high concentrations of monomers of α-synuclein to induce α-synuclein aggregation and phosphorylation[47,48]. This finding suggests that phosphorylated α-synuclein is critical in the pathogenesis of PD[4]. In a recent study, Ramalingam et al. [5] show that neural activity increases pS129 with no change in total α-synuclein. This induction requires action potentials and synaptic transmission, indicating that network activity is responsible for such an effect. Here we show that cells treated with α-synuclein preformed fibrils showed increased levels of pS129 and that IC100 significantly decreased pS129 expression. Moreover, pSer129 expression after IC100 treatment was largely localized near the plasma membrane. It is unclear whether there is a link between proinflammatory signaling and post-translational modifications of α-synuclein. However, a recent study demonstrated that inflammation induced by LPS treatment stimulated α-synuclein phosphorylation at pS129 and accumulation of α-synuclein aggregates that resembled PD-like pathology[49]. Thus, the precise mechanism by which IC100 influences the physiological regulation of α-synuclein phosphorylation at Serine129 and the cellular distribution remains largely undefined.

Our results demonstrate that IC100 significantly blocks inflammasome activation and cytotoxicity in LRRK2 parental RAW 264.7 cells induced by serum-derived and brain-derived ASC specks from PD and LBD, respectively. LRRK2 plays a crucial role in regulating the function of human microglia, primarily by increasing the inflammatory response that potentially contributes to neurodegenerative diseases like PD[1,50]. LRRK2 plays a significant role in regulating inflammasome activation, particularly by promoting the assembly and activity of the NLRC4 inflammasome, leading to increased ASC speck formation and production of IL-1β[51]. Mutations in the LRRK2 gene can exacerbate the aggregation and accumulation of α-synuclein by dysregulating cellular pathways like membrane trafficking and autophagy, ultimately contributing to neuronal damage and neurodegeneration[52–54]. Although LRRK2 cell lines have been valuable for studying Parkinson's disease (PD), they have limitations in that they may not accurately replicate the intricate microglial cellular interactions and microenvironment of the human brain.

In conclusion, this study indicates an association between ASC speck assembly, NLRP1 inflammasome activation, and α-synuclein accumulation in PD. Thus, therapeutics against inflammasomes and ASC specks are promising targets in AD[31,55] and PD[9]. Since IC100 targets inflammasome/ASC specks assembly and activity[29] as well as misfolded protein aggregates, this biologic may be a useful treatment for neurodegeneration in PD.

## Methods

### Postmortem human brains

Informed consent was acquired for postmortem examination research according to the University of Miami, Institutional Regulatory Board (IRB)

guidelines. Research study ethics was obtained from the Human Subjects Research Office, University of Miami, Miami, Florida (IRB ethics number, 19920348 (CR00012340)), Brain Endowment Bank.

### Immunohistochemistry and histochemistry

Standard immunohistochemistry procedures for 20-µm-thick brain sections have been described previously in refs. 56,57. In brief, after deparaffinization, endogenous peroxidase activity was quenched by placing the slides into 3% hydrogen peroxide ($H_2O_2$) for 10 min. Sections were immersed in preheated 10 mM citric acid (VWR, Radnor, PA, USA), pH 6.0, for 30 min and then cooled to room temperature and submerged in formic acid (Sigma–Aldrich, St. Louis, MO, USA) for 5 min. Sections were then blocked in 5% goat serum (Vector Laboratories, Burlingame, Calif., USA) for 20 min before being incubated overnight at 4 °C in a solution of rabbit anti-Phospho-α-Synuclein (Ser129) (D1R1R) antibody (D1R1R; 0.3 µg/mL; Cell Signaling Technologies Danvers, MA, USA), rabbit anti-NLRP3 (3.0 µg/mL; MilliporeSigma, St. Louis, MO, USA), mouse anti-NLRP1 (1.0 µg/mL; Enzo Life Sciences, Farmingdale, NY., USA), or human anti-ASC (IC100, 2 µg/mL; as described in refs. 33,34) in PBS. The next day, sections were exposed to biotinylated horse-anti-mouse IgG, biotinylated goat anti-rabbit IgG secondary antibody (15 µg/mL; Vector Laboratories), or goat anti-human IgG secondary antibody (10 µg/mL; Vector Laboratories) in PBS for 1 h followed by avidin-biotin complex for 1 h (1:200, ABC; Vector Laboratories). Reactions were visualized with 3,3′-diaminobenzidine (MilliporeSigma) for 10 min. Finally, sections were dehydrated, cleared in xylene, and cover-slipped. As a negative control in low AD sections, we performed staining in the absence of the primary antibodies, and no specific staining was identified in these preparations.

### Immunofluorescence labeling

To identify the cellular location of synuclein pathology, microglia, and NLRP1 and NLRP3 proteins, immunofluorescence (IF) triple-labeling was performed on the PD cases and on the control samples. Primary antibodies rabbit anti-NLRP3 (3.0 µg/mL) and mouse anti-NLRP1 (1.0 µg/mL) were mixed in separate cocktail solutions with compatible antibodies, as follows: chicken polyclonal anti-ionized calcium-binding adapter molecule 1 (Iba-1; 0.1 µg/mL) or rabbit polyclonal Iba-1 (0.5 µg/mL; Wako Chemicals) as a marker for microglia and macrophages and mouse monoclonal anti-ASC (B-3; 0.4 µg/ml, Santa Cruz and Biotechnology) or mouse monoclonal anti-α-synuclein (Clone 42; 2.5 µg/ml; BD Transduction) or anti-Phospho-α-synuclein (Ser129). Sections were pretreated as described above and blocked in 5% goat serum for 20 min before the primary antibodies were applied and incubated overnight at 4 °C. Following primary antibody incubation, sections were rinsed three times in PBS for 3 min before the secondary antibodies were added. The samples were finally soaked for 1.5 h in PBS containing secondary antibody cocktail: goat anti-mouse IgG conjugated to Alexa Fluor 488 (4 µg/ml; Invitrogen) or goat anti-rabbit IgG conjugated to Alexa Fluor 488 (4 µg/ml; Invitrogen) and goat anti-human IgG conjugated to Alexa Fluor 546 (4 µg/ml; Invitrogen). Included in the cocktails were goat anti-chicken IgG conjugated to Alexa Fluor 647 (4 µg/ml; Invitrogen). Finally, the sections were cover-slipped using ProLong Gold antifade reagent (Invitrogen) and kept in the dark at 4 °C until analysis.

### Microscopic analyses

Slides containing brain sections that were immunohistochemically stained with anti-ASC (IC100) labeling were scanned over the course of a week using a brightfield slide scanner (MoticEasyScan) at 40× magnification and preset intensity parameters to produce extended depth field images and saved as full-resolution images. Regions of the SN were taken from the SN region of the midbrain, which encompassed an area of 3.0 $mm^2$ per sample using the Image-Pro Premier (Media Cybernetics) program. To ensure that counts included the normally pigmented granular neurons of the SN, neurons that had a cell body of at least 100 $µm^2$ were counted to ensure that these neurons met the criteria. Neurons were sorted using the cell sorting module in Image-Pro Premier. Modular granular neurons with melanin pigment and no ASC (IC100) positivity were counted as "Negative". Neurons with granular ASC positive on the melanin pigment were counted as "Granular" and neurons with minute clumps of ASC staining were counted as "Irregular". Neurons with two or more circular ASC positive accumulations were counted as "Lewy body" and neurons with large pale morphology were counted as, "Pale body." Slides containing brain sections that had been stained with IF techniques were scanned in a singular overnight batch using an Olympus VS120 Slide Scanner at 40× magnification under the same exposure, intensity, and acquisition settings. Full-resolution crops were used for representative images.

### Animals for ASC speck isolation

All animal procedures were approved by the Animal Care and Use Committee of the University of Miami (protocol 21–192 and 22-061). Animal procedures were carried out according to the Guide for the Care and Use of Laboratory Animals (U.S. Public Health). C57BL/6J (strain#000664) and B6.Cg-Gt(ROSA)26Sortm1.1(CAG-Pycard/mCitrine*,-CD2*)Dtg/J (R26-CAG-ASC-citrine; strain#030744[42];) mice were used. 18-month-old and 3-month-old C57BL/6 and 4-month-old R26-CAG-ASC-citrine female mice were sacrificed, and the brain was then removed. Protein lysates were obtained as described in ref. 58 and stored at −80 °C until ASC speck isolation.

### ASC speck isolation

ASC specks were isolated using a combination of partial purification of the pyroptosome, followed by an immunoprecipitation. Protein lysates underwent a modified partial purification of the pyroptosome as described[59]. Briefly, 100 µL lysate was filtered through a 5 µM polyvinylidene difluoride membrane (Millipore) at 2000 × *g* for 5 min. The filtered supernatant was transferred into an Eppendorf tube and centrifuged at 5000 rpm for 8 min. Following removal of the supernatant, the pellet was resuspended in 50 µL CHAPS buffer (Cell Signaling) and centrifuged again at 5000 rpm for 8 min. The supernatant was discarded, and the pellet was resuspended in 27.8 µL CHAPS buffer and 2.2 µL of disuccinimidyl suberate (DSS) (Thermo Fischer Scientific) and left to incubate at room temperature for 30 min.

Following partial purification of the pyroptosome, 2 µL of anti-ASC antibody and 50 µL of Protein G microbeads (Miltenyi Biotec) were incubated with the sample, rotating at 4 °C for 30 min. Samples were diluted with 420 µL CHAPS buffer. M Columns (Miltenyi Biotec) were set up on the OctoMACS™ Magnetic Separator (Miltenyi Biotec) and washed with 250 µL PBS + 1% Triton 100, followed by 100 µL Pierce™ RIPA buffer (Thermo Fischer Scientific). The sample was then added to the column, followed by 3 washes of 500 µL RIPA each. The M column was placed into a collection tube, and 1 mL PBS was added to the column and plunged immediately to elute the ASC specks. The ASC specks were centrifuged at 5000 rpm for 8 min, the supernatant was removed, and the pellet was resuspended in 100 µL PBS. ASC specks were stored at −80 °C. Protein aggregates from the serum of a PD patient (84-year-old female, Hoehn and Yahr Stage 1), the brain of a Lewy body disease patient (83-year-old female with diffuse Lewy body disease, transitional (limbic) type with senile changes), and ASC specks from R26-CAG-ASC-citrine mice were isolated by partial purification of the pyroptosome as described.

### Cell culture

WT microglia were a gift from Dr. Kate Fitzgerald (University of Massachusetts Medical School, Worcester, MA)[60] and were maintained in RPMI 1640 (Gibco) with 10% fetal bovine serum (FBS) and 1% antibiotic-antimycotic (Gibco). HMC3 cells were acquired from ATCC® (CRL-3304™) and were maintained in MEM/EBSS (Cytiva) with 10% FBS. Cells were passaged every 2–3 days once reaching approximately 80−90% confluency. LRRK2 parental RAW 264.7 cells were purchased from ATCC (SC-6003). Cells were grown in culture using Dulbecco's Modified Eagle's Medium with 10% FBS and 1% antibiotic-antimycotic (Gibco).

### Activation of the inflammasome *via* LPS and ATP

To activate the inflammasome to stimulate the release of ASC specks, HMC3 cells were seeded at 10,000 cells/well in a 96-well plate and left to adhere overnight. Wells were treated with 200 ng/mL of lipopolysaccharide-EB (LPS-EB) (InvivoGen) for 24 h followed by the addition of adenosine triphosphate (ATP) (Thermo Fischer Scientific) to a concentration of 5 mM and incubated for an additional 30 min. A group of cells was pretreated with 5 μg/mL IC100 for 1 h before ATP administration. Media was stored at −80 °C if not analyzed immediately.

### Measurement of ASC concentration

2 μL of the media from control, LPS + ATP activated, and LPS + ATP activated with IC100 pretreatment was administered to the NanoQuant plate for the SPARK® 10 M spectrophotometer (Tecan) in duplicate, and absorbance was read at 280 nm to determine protein concentration. The absorption coefficient was calculated on https://web.expasy.org/protparam/ based on the amino acid sequence of ASC[61]. Accordingly, raw values were averaged, then multiplied by 20 and divided by 0.673 to determine the concentration of ASC in μg/μL.

### Administration of ASC specks to microglia

WT microglia were seeded at 10,000 cells/well in a 96-well plate and left to adhere overnight; ASC specks isolated from C57BL/6 mice were administered increasing doses from 3 to 300 μg/mL and incubated for 4 h. HMC3 cells were seeded at 100,000 cells in a chamber slide and left to adhere overnight; ASC specks isolated from R26-CAG-ASC-citrine mice were administered at a concentration of 265 μg/mL for 1.5 h. If the media were not analyzed directly after stimulation, it was stored at −80 °C until analysis.

### Caspase-1 activity assay

Caspase-1 activity was measured using the Caspase-Glo® 1 Inflammasome Assay (Promega) following the manufacturer's instructions. Briefly, 50 μL of cell media was transferred to a white 96-well plate with a transparent bottom, and then 50 μL of Caspase-Glo® 1 Reagent was added. The plate was covered with a plate sealer and shaken on a plate shaker for 30 s. The plate was incubated in the dark for 1 h, then measured for luminescence with the SPARK® 10M spectrophotometer (Tecan).

### ECLIA for IL-1β assay

IL-1β from the media of cells stimulated with synuclein fibers was analyzed by ECLIA using a V-Plex IL-1β assay kit (MSD) according to the manufacturer's instructions as described in ref. 62.

### Cell death assay

Cell death was measured using the Lactate Dehydrogenase (LDH) Release Assay (Promega) following the manufacturer's instructions. Briefly, 50 μL of cell media was transferred to a transparent 96-well plate, and 50 μL of the CytoTox 96® Reagent was added. The plate was incubated in the dark for 30 min, then 50 μL of Stop Solution was added. Absorbance was read at 490 nm with the SPARK® 10M spectrophotometer (Tecan).

### α-synuclein assembly and generation

Human α-synuclein was purchased from ND Biosciences. To assemble α-synuclein into fibrils, the monomeric form of the protein was diluted in 50 mM Tris-HCl (pH 7.5) and 150 mM KCl to 1 mg/mL and placed in a temperature-controlled shaker to mix at 37 °C for 5 days in order to achieve fibrillary conformation. Aliquots were then obtained on different days to perform a ThT assay by mixing the aliquots with Thioflavin T at a final concentration of 10 μM. Reaction was then read in the SPARK® 10M spectrophotometer (Tecan, Männedorf, Switzerland) using an excitation wavelength of 440 nm and an emission wavelength of 482 nm. α-synuclein assembly was also evaluated by immunoblot analysis as described above. The α-synuclein fibrils were stored at −80 °C and used at a concentration of 7 μM.

### Microglial uptake of ASC specks

After administration of ASC specks, the media was aspirated, and the chamber was washed with 2 mL PBS. Three μL of CellMask™ Plasma Membrane Stain (Invitrogen) were added to 2 mL of media and added to the chamber of a chamber slide. The slide was incubated for 10 min at 37 °C with 5% $CO_2$. The staining solution was aspirated, and 1 mL of BD CytoFix™ Fixation Buffer (BD Biosciences) was added and incubated for 10 min at 37 °C with 5% $CO_2$. The fixation solution was aspirated, and the chamber was washed 3 times with 2 mL PBS each. Chambers were then removed, and the slide was cover-slipped with VECTASHIELD® HardSet™ Antifade Mounting Medium with DAPI (Vector Laboratories). The slide was imaged with the Dragonfly 200 spinning disk confocal system (Andor).

### Microglia treatment with α-synuclein fibrils

HM3C cells were plated at approximately $1 \times 10^5$ cells/well in 12-well flat-bottom tissue culture dishes. After 24 h in culture, one group of cells was treated with α-synuclein fibrils (7 mM), while controls were left untreated. To determine the effects of IC100 on α-synuclein expression, HMC3 cells received 10 μg/mL of IC100 for 1 h, and then 7 μM of α-synuclein preformed fibrils were added to each well and grown for 3 days at 37 °C. To assess whether IC100 interfered with inflammasome activation, HMC3 cells were primed with LPS for 4 h and then treated with 7 μM of α-synuclein preformed fibrils or treated with IC100 (10 μg/mL) for 24 h. Cells were washed twice in PBS, lysed, and caspase-1 activity was measured using the Caspase-Glo assay following the manufacturer's protocol as described above.

### Immunoblot analysis

For protein lysate collection, HMC3 cells were washed in cold PBS and then lysed in protein extraction buffer containing protease inhibitor cocktail (Sigma–Aldrich, St Lois, MO, USA)[58] by scraping off the wells. Cells in the extraction buffer were then centrifuged for 3 min at 10,000 × *g*. The supernatant was then used for immunoblotting procedures, and the pellet was discarded. For immunoblotting, protein lysates were resolved as described in ref. 58 using antibodies (1:1000 dilution) against phospho-α-synuclein (Ser129) (Cell Signaling), Total-α-synuclein (Cell Signaling), and β-actin (Sigma) as described[58]. Polyvinylidene difluoride (PVDF) membranes were imaged using the ChemiDoc Touch Imaging System (Bio-Rad). All blots or gels were derived from the same experiment and were processed in parallel.

### Statistical analyses

After identification of outliers by the ROUT method ($Q = 1\%$) and removal of the identified outliers, descriptive statistics were obtained. Normality was determined by the Shapiro–Wilk test. Comparisons between more than 2 groups for parametric data were done by a one-way ANOVA, followed by Dunnett's multiple comparison test or a Holm–Šídák's multiple comparisons test. For non-parametric data, a Kruskal–Wallis test followed by Dunn's multiple comparison test was used. For comparison between 2 groups for parametric data, an unpaired *t*-test was carried out. Statistical Analyses were done using Prism 10.0 (GraphPad).

### Immunocytochemistry and confocal microscopy

HM3C cells were plated in two-well chamber slides at approximately $1 \times 10^4$ cells/well. After 24 h in culture, one group of cells was treated with α-synuclein fibrils (7 μM) alone, while controls were left untreated. To determine the effects of IC100 on α-synuclein expression, HMC3 cells received 10 μg/mL of IC100 for 1 h, and then 7 μM of α-synuclein fibrils were added to each well and grown for 3 days at 37 °C and fixed in 10% buffered formalin for immunohistochemistry and confocal microscopy. After fixation, cells were permeabilized with 1% Triton X-100 in PBS for 20 min, washed 3× in cold PBS, and blocked in PBS containing 5% goat serum. Cells were stained with primary antibodies, rabbit monoclonal antibody against phospho-a-synuclein (Ser129) (Cell Signaling cat no. #23706, 1:500) or mouse monoclonal anti-ASC (1:1000, Santa Cruz, sc-

271054, 1:500) overnight at 4 °C. Cells were washed in PBS 3× and counterstained with secondary antibodies, donkey anti-rabbit IgG conjugated to Alexa Fluor 488 (InVitrogen, cat. No. 821206, 1:1000) or goat anti-mouse IgG conjugated to Alexa Fluor 594 (ThermoFisher Scientific, cat. No. A-11005, 1:1000). The slides were cover-slipped with VECTASHIELD® HardSet™ Antifade Mounting Medium with DAPI (Vector Laboratories) and kept in the dark until imaging with the Dragonfly 200 spinning disk confocal system (Andor, MA).

## Data availability

The raw data supporting the conclusions of this article will be made available by the authors without undue reservation.

Received: 12 August 2024; Accepted: 8 April 2025;
Published online: 25 April 2025

## References

1. Jewell, S., Herath, A. M. & Gordon, R. Inflammasome activation in Parkinson's disease. *J. Parkinsons Dis.* **12**, S113–S128 (2022).
2. Heneka, M. T., McManus, R. M. & Latz, E. Inflammasome signalling in brain function and neurodegenerative disease. *Nat. Rev. Neurosci.* **19**, 610–621 (2018).
3. Heneka, M. T. et al. NLRP3 is activated in Alzheimer's disease and contributes to pathology in APP/PS1 mice. *Nature* **493**, 674–678 (2013).
4. Fujiwara, H. et al. alpha-Synuclein is phosphorylated in synucleinopathy lesions. *Nat. Cell Biol.* **4**, 160–164 (2002).
5. Ramalingam, N. et al. Dynamic physiological alpha-synuclein S129 phosphorylation is driven by neuronal activity. *NPJ Parkinsons Dis.* **9**, 4 (2023).
6. Attems, J. et al. Neuropathological consensus criteria for the evaluation of Lewy pathology in post-mortem brains: a multi-centre study. *Acta Neuropathol.* **141**, 159–172 (2021).
7. Wakabayashi, K. et al. The Lewy body in Parkinson's disease and related neurodegenerative disorders. *Mol. Neurobiol.* **47**, 495–508 (2013).
8. Ising, C. et al. NLRP3 inflammasome activation drives tau pathology. *Nature* **575**, 669–673 (2019).
9. Gordon, R. et al. Inflammasome inhibition prevents alpha-synuclein pathology and dopaminergic neurodegeneration in mice. *Sci. Transl. Med.* **10**, eaah4066 (2018).
10. von Herrmann, K. M. et al. NLRP3 expression in mesencephalic neurons and characterization of a rare NLRP3 polymorphism associated with decreased risk of Parkinson's disease. *NPJ Parkinsons Dis.* **4**, 24 (2018).
11. Anderson, F. L. et al. Plasma-borne indicators of inflammasome activity in Parkinson's disease patients. *NPJ Parkinsons Dis.* **7**, 2 (2021).
12. Chatterjee, K. et al. Inflammasome and alpha-synuclein in Parkinson's disease: a cross-sectional study. *J. Neuroimmunol.* **338**, 577089 (2020).
13. Cabrera Ranaldi, E. et al. Proof-of-principle study of inflammasome signaling proteins as diagnostic biomarkers of the inflammatory response in Parkinson's disease. *Pharmaceuticals* **16**, 883 (2023).
14. Wang, X. et al. alpha-synuclein promotes progression of Parkinson's disease by upregulating autophagy signaling pathway to activate NLRP3 inflammasome. *Exp. Ther. Med.* **19**, 931–938 (2020).
15. Dick, M. S., Sborgi, L., Ruhl, S., Hiller, S. & Broz, P. ASC filament formation serves as a signal amplification mechanism for inflammasomes. *Nat. Commun.* **7**, 11929 (2016).
16. Franklin, B. S. et al. The adaptor ASC has extracellular and 'prionoid' activities that propagate inflammation. *Nat. Immunol.* **15**, 727–737 (2014).
17. Choi, I. et al. Microglia clear neuron-released alpha-synuclein via selective autophagy and prevent neurodegeneration. *Nat. Commun.* **11**, 1386 (2020).
18. Zhang, W. et al. Aggregated alpha-synuclein activates microglia: a process leading to disease progression in Parkinson's disease. *FASEB J.* **19**, 533–542 (2005).
19. Minami, S. S. et al. Selective targeting of microglia by quantum dots. *J. Neuroinflamm.* **9**, 22 (2012).
20. Awa, S. et al. Phosphorylation of endogenous alpha-synuclein induced by extracellular seeds initiates at the pre-synaptic region and spreads to the cell body. *Sci. Rep.* **12**, 1163 (2022).
21. Niskanen, J. et al. Uptake of alpha-synuclein preformed fibrils is suppressed by inflammation and induces an aberrant phenotype in human microglia. *Glia.* **73**, 159–174 (2024).
22. Scheiblich, H. et al. Microglia jointly degrade fibrillar alpha-synuclein cargo by distribution through tunneling nanotubes. *Cell* **184**, 5089–5106.e5021 (2021).
23. Stefanova, N. Microglia in Parkinson's disease. *J. Parkinsons Dis.* **12**, S105–S112 (2022).
24. Huang, S. et al. A selective NLRP3 inflammasome inhibitor attenuates behavioral deficits and neuroinflammation in a mouse model of Parkinson's disease. *J. Neuroimmunol.* **354**, 577543 (2021).
25. Qiu, X. et al. Inhibition of NLRP3 inflammasome by glibenclamide attenuated dopaminergic neurodegeneration and motor deficits in paraquat and maneb-induced mouse Parkinson's disease model. *Toxicol. Lett.* **349**, 1–11 (2021).
26. Shim, D. W. et al. BOT-4-one attenuates NLRP3 inflammasome activation: NLRP3 alkylation leading to the regulation of its ATPase activity and ubiquitination. *Sci. Rep.* **7**, 15020 (2017).
27. Baroja-Mazo, A. et al. The NLRP3 inflammasome is released as a particulate danger signal that amplifies the inflammatory response. *Nat. Immunol.* **15**, 738–748 (2014).
28. Lonnemann, N. et al. The NLRP3 inflammasome inhibitor OLT1177 rescues cognitive impairment in a mouse model of Alzheimer's disease. *Proc. Natl Acad. Sci. USA* **117**, 32145–32154 (2020).
29. de Rivero Vaccari, J. P. et al. Mechanism of action of IC 100, a humanized IgG4 monoclonal antibody targeting apoptosis-associated speck-like protein containing a caspase recruitment domain (ASC). *Transl. Res.* **251**, 27–40 (2023).
30. de Rivero Vaccari, J. P., Lotocki, G., Marcillo, A. E., Dietrich, W. D. & Keane, R. W. A molecular platform in neurons regulates inflammation after spinal cord injury. *J. Neurosci.* **28**, 3404–3414 (2008).
31. Johnson, N. H., de Rivero Vaccari, J. P., Bramlett, H. M., Keane, R. W. & Dietrich, W. D. Inflammasome activation in traumatic brain injury and Alzheimer's disease. *Transl. Res.* **254**, 1–12 (2023).
32. Kerr, N. A. et al. Traumatic brain injury-induced acute lung injury: evidence for activation and inhibition of a neural-respiratory-inflammasome axis. *J. Neurotrauma* **35**, 2067–2076 (2018).
33. Desu, H. L. et al. IC100: a novel anti-ASC monoclonal antibody improves functional outcomes in an animal model of multiple sclerosis. *J. Neuroinflamm.* **17**, 143 (2020).
34. Cyr, B., Hadad, R., Keane, R. W. & de Rivero Vaccari, J. P. The Role of Non-canonical and Canonical Inflammasomes in Inflammaging. *Front. Mol. Neurosci.* **15**, 774014 (2022).
35. Vontell, R. T. et al. Identification of inflammasome signaling proteins in neurons and microglia in early and intermediate stages of Alzheimer's disease. *Brain Pathol.* **33**, e13142 (2023).
36. Wang, W. et al. Caspase-1 causes truncation and aggregation of the Parkinson's disease-associated protein alpha-synuclein. *Proc. Natl Acad. Sci. USA* **113**, 9587–9592 (2016).
37. Hulse, J. & Bhaskar, K. Crosstalk between the NLRP3 inflammasome/ASC speck and amyloid protein aggregates drives disease progression in Alzheimer's and Parkinson's disease. *Front. Mol. Neurosci.* **15**, 805169 (2022).
38. Codolo, G. et al. Triggering of inflammasome by aggregated alpha-synuclein, an inflammatory response in synucleinopathies. *PLoS ONE* **8**, e55375 (2013).
39. Kouli, A., Horne, C. B. & Williams-Gray, C. H. Toll-like receptors and their therapeutic potential in Parkinson's disease and alpha-synucleinopathies. *Brain Behav. Immun.* **81**, 41–51 (2019).

40. Zheng, R. et al. ASC specks exacerbate alpha-synuclein pathology via amplifying NLRP3 inflammasome activities. *J. Neuroinflamm.* **20**, 26 (2023).
41. Rocha Cabrero, F. & Morrison, E. H. Lewy bodies. In *StatPearls* (Treasure Island, FL, 2024).
42. Tzeng, T. C. et al. A fluorescent reporter mouse for inflammasome assembly demonstrates an important role for cell-bound and free ASC specks during in vivo infection. *Cell Rep.* **16**, 571–582 (2016).
43. Gluck, I. M. et al. Nanoscale organization of the endogenous ASC speck. *iScience* **26**, 108382 (2023).
44. Sahillioglu, A. C. & Ozoren, N. Artificial loading of ASC specks with cytosolic antigens. *PLoS ONE* **10**, e0134912 (2015).
45. Kontaxi, C., Kim, N. & Cousin, M. A. The phospho-regulated amphiphysin/endophilin interaction is required for synaptic vesicle endocytosis. *J. Neurochem.* **166**, 248–264 (2023).
46. Mao, X. et al. Pathological alpha-synuclein transmission initiated by binding lymphocyte-activation gene 3. *Science* **353**, aah3374 (2016).
47. Henderson, M. X. et al. Spread of alpha-synuclein pathology through the brain connectome is modulated by selective vulnerability and predicted by network analysis. *Nat. Neurosci.* **22**, 1248–1257 (2019).
48. Courte, J. et al. The expression level of alpha-synuclein in different neuronal populations is the primary determinant of its prion-like seeding. *Sci. Rep.* **10**, 4895 (2020).
49. Niu, H. et al. IL-1beta/IL-1R1 signaling induced by intranasal lipopolysaccharide infusion regulates alpha-Synuclein pathology in the olfactory bulb, substantia nigra and striatum. *Brain Pathol.* **30**, 1102–1118 (2020).
50. Taymans, J. M. et al. Perspective on the current state of the LRRK2 field. *NPJ Parkinsons Dis.* **9**, 104 (2023).
51. Liu, W. et al. LRRK2 promotes the activation of NLRC4 inflammasome during Salmonella Typhimurium infection. *J. Exp. Med.* **214**, 3051–3066 (2017).
52. Lin, X. et al. Leucine-rich repeat kinase 2 regulates the progression of neuropathology induced by Parkinson's-disease-related mutant alpha-synuclein. *Neuron* **64**, 807–827 (2009).
53. Daher, J. P., Volpicelli-Daley, L. A., Blackburn, J. P., Moehle, M. S. & West, A. B. Abrogation of alpha-synuclein-mediated dopaminergic neurodegeneration in LRRK2-deficient rats. *Proc. Natl Acad. Sci. USA* **111**, 9289–9294 (2014).
54. Oun, A. et al. The multifaceted role of LRRK2 in Parkinson's disease: from human iPSC to organoids. *Neurobiol. Dis.* **173**, 105837 (2022).
55. Dempsey, C. et al. Inhibiting the NLRP3 inflammasome with MCC950 promotes non-phlogistic clearance of amyloid-beta and cognitive function in APP/PS1 mice. *Brain Behav. Immun.* **61**, 306–316 (2017).
56. Vontell, R. et al. Toll-like receptor 3 expression in glia and neurons alters in response to white matter injury in preterm infants. *Dev. Neurosci.* **35**, 130–139 (2013).
57. Vontell, R. et al. Cellular mechanisms of toll-like receptor-3 activation in the thalamus are associated with white matter injury in the developing brain. *J. Neuropathol. Exp. Neurol.* **74**, 273–285 (2015).
58. Cyr, B. & de Rivero Vaccari, J. P. Methods to study inflammasome activation in the central nervous system: immunoblotting and immunohistochemistry. In *NLR Proteins: Methods and Protocols* (eds. Pelegrín, P. & Di Virgilio, F.) 223–238 (Springer US, New York, NY, 2023).
59. Fernandes-Alnemri, T. & Alnemri, E. S. Assembly, purification, and assay of the activity of the ASC pyroptosome. *Methods Enzymol.* **442**, 251–270 (2008).
60. Halle, A. et al. The NALP3 inflammasome is involved in the innate immune response to amyloid-β. *Nat. Immunol.* **9**, 857–865 (2008).
61. Gasteiger, E. et al. Protein identification and analysis tools on the ExPASy server. In *The Proteomics Protocols Handbook* (ed. Walker, J. M.) 571–607 (Humana Press, Totowa, NJ, 2005).
62. Cyr, B. & de Rivero Vaccari, J. P. Sex differences in the inflammatory profile in the brain of young and aged mice. *Cells* **12**, 1372 (2023).


## Acknowledgements

This research was funded by a grant from the Michael J. Fox Foundation to ZyVersa Therapeutics Inc. and the University of Miami to R.W.K. and J.P.d.R.V. (MJFF-021165).

## Author contributions

R.W.K., J.P.d.R.V., R.T.V., and B.C. conceptualized and designed the study. R.T.V., B.C, R.H., J.P.d.R.V., and R.W.K. performed data analysis. R.H. and B.C. provided input in the study plan and analyses. B.C., R.H., R.T.V., J.P.d.R.V., and R.W.K. wrote the first draft of the manuscript. B.R., R.H., R.W.K. performed cell culturing and immunoblotting procedures. J.P.d.R.V. and R.H. performed ELICA analysis. B.R., R.H., and J.P.d.R.V. isolated and analyzed ASC specks from serum and tissues. R.T.V. and J.P.R.V. obtained and analyzed Parkinson's disease and Lewy body disease patient samples. R.T.V., R.H., and R.W.K. performed the immunohistochemical staining and confocal analysis. R.W.K., R.V.T., and J.P.d.R.V. supervised the project. B.C, R.T.V., and H.D. contributed equally to this work. All authors critically reviewed the manuscript, and R.W.K., J.P.d.R.V., and R.V.T. edited the manuscript.

## Competing interests

J.P.d.R.V. and R.W.K. are co-founders and managing members of InflaMaCORE, LLC, and have licensed patents on inflammasome proteins as biomarkers of injury and disease, as well as on targeting inflammasome proteins for therapeutic purposes. J.P.d.R.V. and R.W.K. are Scientific Advisory Board Members of ZyVersa Therapeutics Inc. ZyVersa Therapeutics holds licensed patents on IC100 as a therapy against inflammasome-related diseases.

## Additional information

**Supplementary information** The online version contains supplementary material available at https://doi.org/10.1038/s41531-025-00963-8.

**Correspondence** and requests for materials should be addressed to Robert W. Keane.